Redox Biology 41 (2021) 101913

Contents lists available at ScienceDirect

Redox Biology

journal homepage: www.elsevier.com/locate/redox

Endogenous generation of nitro-fatty acid hybrids having dual nitrate ester ($RONO_2$) and nitroalkene (RNO_2) substituents

Marco Fazzari [a,*], Steven R. Woodcock [a], Pascal Rowart [a], Karina Ricart [b], Jack R. Lancaster Jr. [a,c], Rakesh Patel [b], Dario A. Vitturi [a,c,d], Bruce A. Freeman [a], Francisco J. Schopfer [a,c]

[a] Department of Pharmacology and Chemical Biology, University of Pittsburgh, 200 Lothrop Street, Pittsburgh, 15261, PA, USA
[b] Department of Pathology, University of Alabama, 901 19th Street South, Birmingham, 35294, AL, USA
[c] Pittsburgh Heart, Lung, Blood, and Vascular Medicine Institute, Pittsburgh, 15213, PA, USA
[d] Center for Critical Care Nephrology, Pittsburgh, 15213, PA, USA

ARTICLE INFO

Keywords:
Nitro-nitrate-fatty acid
Nitro-conjugated linoleic acid
Conjugated linoleic acid
Fatty acid nitroalkene
Nitrate ester

ABSTRACT

Organic nitrate esters, long-recognized therapies for cardiovascular disorders, have not been detected biologically. We characterize in rat stomach unsaturated fatty acid nitration reactions that proceed by generation of nitro-nitrate intermediates (NO_2–ONO_2-FA) via oxygen and nitrite dependent reactions. NO_2–ONO_2-lipids represent ~70% of all nitrated lipids in the stomach and they decay *in vitro* at neutral or basic pH by the loss of the nitrate ester group (-ONO_2) from the carbon backbone upon deprotonation of the α-carbon (pKa ~7), yielding nitrate, nitrite, nitrosative species, and an electrophilic fatty acid nitroalkene product (NO_2-FA). Of note, NO_2-FA are anti-inflammatory and tissue-protective signaling mediators, which are undergoing Phase II trials for the treatment of kidney and pulmonary diseases. The decay of NO_2–ONO_2-FA occurs during intestinal transit and absorption, leading to the formation of NO_2-FA that were subsequently detected in circulating plasma triglycerides. These observations provide new insight into unsaturated fatty acid nitration mechanisms, identify nitro-nitrate ester-containing lipids as intermediates in the formation of both secondary nitrogen oxides and electrophilic fatty acid nitroalkenes, and expand the scope of endogenous products stemming from metabolic reactions of nitrogen oxides.

1. Introduction

The chemical synthesis of nitroglycerin (NTG) in 1846 by Ascanio Sobrero led to the initial manufacturing of this nitrate ester and its use in mining and warfare. Upon the 1879 description of NTG's therapeutic effects in angina pectoris, extensive use of nitrate esters in cardiovascular medicine has continued to the present. After discovering the endogenous generation of nitric oxide ($^{\bullet}NO$) and its role in endothelium-dependent vascular relaxation in 1986, it is now appreciated that diverse inflammatory and metabolic reactions give rise to a broad array of chemically-reactive nitrogen oxides and oxygen-derived oxidizing, nitrosating, and nitrating signaling mediators [1,2]. The class of endogenous mediators described herein stems from diverse reactions induced by the primary species $^{\bullet}NO$, nitrite (NO_2^-), superoxide ($O_2^{\bullet-}$), and hydrogen peroxide (H_2O_2). These reactive species undergo both non-enzymatic and enzyme-catalyzed reduction-oxidation (redox) reactions that have in common the generation of the nitrating species nitrogen dioxide ($^{\bullet}NO_2$) [3–5]. One example of redox-induced $^{\bullet}NO_2$ generation comes from the protonation of NO_2^- during digestion or inflammation. The latter generates both symmetric and asymmetric dinitrogen trioxide (N_2O_3) that, upon homolytic cleavage, yields $^{\bullet}NO$ and $^{\bullet}NO_2$ [6]. Another example is the reaction between $O_2^{\bullet-}$ and $^{\bullet}NO$ and the consequent formation of peroxynitrite ($ONOO^-$), which in turn yields $^{\bullet}NO_2$ either from protonation and homolysis (also producing hydroxyl radical, $^{\bullet}OH$) [7] or reaction with CO_2 (also producing carbonate anion radical, $CO_3^{\bullet-}$) [8]. Other sources of $^{\bullet}NO_2$ are the autoxidation of $^{\bullet}NO$ [9] and the myeloperoxidase-induced oxidation of NO_2^- [10,11]. These redox reactions induce nitration of guanine, tyrosine, tryptophan, and conjugated fatty acids, the latter promoting the endogenous formation of fatty acid nitro-alkenes (NO_2-FA) in plants and

* Corresponding author. Dept. of Pharmacology and Chemical Biology, University of Pittsburgh, 200 Lothrop Street, Pittsburgh, 15261, PA, USA
E-mail address: maf167@pitt.edu (M. Fazzari).

https://doi.org/10.1016/j.redox.2021.101913
Received 22 January 2021; Received in revised form 15 February 2021; Accepted 18 February 2021
Available online 24 February 2021

mammals [12–15]. Electrophilic NO_2-FA reversibly alkylate soft nucleophilic amino acids, thus post-translationally modifying (PTM) functionally-significant cysteines in enzymes and transcriptional regulatory proteins [16]. This reversible protein thiol alkylation by hydrophobic fatty acid nitroalkenes, as well as myristate, palmitate, isoprenes, and other lipids, induces a panoply of protein distribution, cell signaling, and gene expression responses [5,16–19].

The reactions of photochemical air pollutants $^{\bullet}NO$ and $^{\bullet}NO_2$, delivered in reagent quantities as gases, have shown that the nitration of esterified monounsaturated and bis-allylic fatty acid dienes yield multiple oxidation products, including nitro-nitrate (NO_2–ONO_2) derivatives [20]. In healthy humans, the oral supplementation of conjugated diene-containing linoleic acid (CLA) and $^{15}NO_2^-$ or $^{15}NO_3^-$ resulted in nM concentrations of $^{15}NO_2$-CLA in plasma and urine [21]. Still, to date, no nitrate ester derivatives of lipids, carbohydrates, nucleotides, or other biomolecules have been detected *in vivo* [22–24]. To test this possibility, the products of CLA nitration during digestion were evaluated. Herein, we report that the *in vitro* and *in vivo* nitration of unsaturated fatty acids proceeds through the formation of an organic nitrate-containing intermediate that stabilizes the initial radical formed upon addition of $^{\bullet}NO_2$ to a conjugated diene. Specifically, NO_2–ONO_2-CLA derivatives were endogenously generated under acidic gastric conditions after oral supplementation of dietary levels of CLA and NO_2^-. NO_2–ONO_2-CLA species are non-electrophilic and decompose at physiological pH to the electrophilic nitroalkene NO_2-CLA in concert with the generation of secondary reactive nitrogen oxide species.

2. Materials and methods

9- and 12-nitro-octadeca-9,11-dienoic acid (9-NO_2-CLA and 12-NO_2-CLA), and the corresponding isotopically labeled internal standard ([^{15}N]O_2-CLA), and 10-nitro-stearic acid (NO_2-SA) standard were synthesized and quantitated as previously described [25–27]. The abbreviation NO_2-CLA refers to a mixture of the above-mentioned positional isomers. 9,11 and 10,12 mixed isomers of octadecadienoic acid (CLA) (UC-59AX) and 1,2-dipalmitoylglycerol (D-151) were purchased from Nu-Check (Elysian, MN, USA) to synthesize dipalmitoyl-CLA glycerol standard (CLA-TAG) as reported before [28]. For *in vitro* assays octadeca-9Z,11E-dienoic acid was purchased from Cayman Chemical (Ann Arbor, MI, USA). Gastric juice artificial (S76772) was from Fisher Scientific Company. Chemicals were analytical grade and purchased from Sigma (St. Louis, MO) unless otherwise stated. Solvents used for extractions and mass spectrometric analyses were from Burdick and Jackson (Muskegon, MI).

2.1. Synthesis of NO_2-CLA-containing TAG standard

Synthesis of NO_2-CLA-TAG was performed by nitration of CLA-TAG. Briefly, an oven-dried 20 mL vial was charged with CLA-TAG (87 mg) in 5 mL CH_2Cl_2. Trifluoroacetic anhydride (150 μL) and tetrabutylammonium acetate (57 mg) were added to the stirred solution under nitrogen. The vial was stirred for 10 min and then 10 μL hydrofluoroboric acid (48% aq.) were added. The vial was sealed, covered in aluminum foil and the solution stirred at room temperature overnight. The next day, the solution was quenched and partitioned with 5 mL water, transferred to a separatory funnel, and the aqueous layer was extracted 3 × CH_2Cl_2. The organic layers were combined, washed 1 × water and 1 × brine, then dried over anhydrous sodium sulfate. The solids were filtered, and the solvent removed by rotary evaporation, transferred to a new 20 mL vial, and redissolved in 10 mL dry Et_2O. Potassium proprionate (135 mg) was added to the stirred solution and the resulting suspension stirred at room temperature overnight. The next day the solution was partitioned with 5 mL 0.1M HCl, stirred briefly, then extracted three times with 5 mL Et_2O. The organic layers were washed with water and brine, then dried over sodium sulfate. The solvents were removed by rotary evaporation and the resulting oil purified by column chromatography (silica gel, 0–8% EtOAc/hexanes) to yield 66 mg of a light-yellow oil (72%). Products were analyzed by HPLC-HR-MS/MS, 1H NMR, and 13C NMR for structural confirmation (Suppl. Fig. 1B, C, D).

^{1}H NMR (600 MHz, $CDCl_3$) δ (ppm): 7.52 (-C*H*=CNO_2, d, J = 11.4 Hz, 1H); 6.32 (CH_2–C*H*=CH, dt, J = 14.9, 7.2 Hz, 1H); 6.19 (CH=C*H*–CH=, dd, J = 13.8, 12.9 Hz, 1H); 5.24 (CH_2-*H*C(OR)-CH_2, quint, J = 4.8 Hz, 1H); 4.28 (CH_2–C*H*(OR)CH_2, dd, J = 11.9, 3.7 Hz, 2H); 4.14 (CH_2–CH(OR)CH_2, dd, J = 11.9, 5.9 Hz, 2H); 2.64 (CNO_2–CH_2, t, J = 7.6 Hz, 2H); 2.30 (CH_2–CO_2, t, J = 7.5 Hz, 6H); 2.23 (CH_2–CH=CH, 2H); 1.59 (m, 7H); 1.50 (m, 3H); 1.44 (m, 2H); 1.30 - 1.24 (br m, 55H); 0.86 (-CH_3, t, J = 7.0 Hz, 9H).

^{13}C (150 MHz, $CDCl_3$) δ (ppm): 172.7, 149.0, 148.9, 133.7, 123.5, 68.9, 62.0, 34.0, 31.9, 31.6, 29.7, 29.6, 29.6, 29.6, 29.4, 29.3, 29.2, 29.0, 24.8, 22.7, 22.6, 14.1 (note only representational peaks reported from isomeric multiplets).

2.2. Animal study

Male Sprague-Dawley rats (~250 g, 9–10 weeks old, n = 3 per group) were fasted overnight and treated with pentagastrin (200 μg/Kg, *i.p.*) to stimulate gastric acid secretion. After 1 hr, rats were gavaged with 17.2 mg/kg synthetic CLA-TAG standard and 4.4 mg/kg $NaNO_2$ dissolved in polyethylene glycol 400. To assess the CLA-TAG products formed in the stomach, one group of rats was euthanized after 45 min and gastric content was collected and processed as reported below. To evaluate the plasma distribution of gastric CLA-TAG products, nine rats were randomly divided into three groups and orally supplemented at the same concentrations as above with: 1) CLA-TAG + $NaNO_2$, 2) CLA-TAG, and 3) $NaNO_2$. After 40 min, rats were treated with orlistat 2 mg/Kg (*i.v.*) and blood was collected at 1, 2, 4 hr, centrifuged, and the plasma was stored at −80 °C until used. Animal studies were performed in accordance with the Guide for the Care and Use of Laboratory Animals published by the United States National Institutes of Health (NIH Publication No.85-23, revised 1996).

2.3. Analysis of gastric and plasma CLA-TAG products

The gastric content was diluted with 2 mL saline, and reaction products were extracted with 2 mL hexane, dried under a stream of nitrogen gas, dissolved in 1 mL ethyl acetate and analyzed by HPLC-HR-MS.

Plasma samples were spiked with 250 pmol internal standard [^{15}N]O_2-CLA in presence of 10 μL sulfanilamide (10% w/v acetonitrile) to avoid any potential artifactual nitration during acidic extraction. Lipids were extracted with 200 μL hexane/isopropanol/1 M formic acid (30:20:2, v/v/v) followed by addition of an equal volume of hexane, vortexing, and centrifugation at 2000 g for 5 min at 4 °C. The upper organic phase was recovered, dried under nitrogen, and reconstituted in 100 μL acetonitrile before HPLC-MS/MS analysis. This method allowed to analyze free concentrations of NO_2-CLA while its esterified levels were measured using an acid hydrolysis method with minor modifications as previously [27]. Briefly, plasma (25 μL) spiked with 2.5 pmol internal standard [^{15}N]O_2-CLA was incubated with 1 mL acetonitrile/HCl (9:1, v/v), in presence of 10 μL sulfanilamide at 90 °C for 1 hr. After incubation, 1 mL saline was added followed by 2 mL hexane, and samples were vortexed and centrifuged at 2000 *g* for 5 min at 4 °C. Then, the hexane phase was dried under a nitrogen stream and reconstituted in acetonitrile for HPLC-MS/MS analysis. The esterified levels of NO_2-CLA were obtained by subtracting the free acid levels (hexane/isopropanol/1 M formic acid extracts) from the total levels (after hydrolysis condition).

2.4. Analysis of gastric and base-catalyzed decay CLA products

Independent reactions of free CLA or CLA-TAG standards (0.5 mg) with 2 mM $NaNO_2$ were performed in pre-warmed artificial gastric juice

for 1 hr at 37 °C under continuous magnetic agitation in aerobic conditions or in glovebox with a 2–4% H_2 atmosphere of catalyst-deoxygenated nitrogen (anaerobic conditions). Then, *in vitro* gastric products were extracted with 1 mL hexane, dried in a stream of nitrogen, dissolved into 150 μL isopropanol/acetonitrile (1/1, v/v), and analyzed by HPLC-DAD-Uv-Vis before and after base-catalyzed degradation with 5 μL ammonium hydroxide (NH_4OH). Relative quantitation was reported as percentage of the total areas recorded for all peaks in the chromatogram. Further characterization of gastric products before and after alkaline decomposition was performed collecting Uv–Vis fractions followed by HPLC-HR-MS analysis.

UV–Vis decay kinetics were performed using 50 μL hexane extracts, which were dried under nitrogen, resuspended into 300 μL methanol and analyzed at 312 nm by UV–Vis spectrophotometry before and after addition of 3 μL phosphate buffers at pH ranging from 5.8 to 9. Then, initial rate of each kinetic was normalized as rate % of maximum and plotted versus pH to describe a sigmoid, which inflection point corresponded to the pKa of NO_2–ONO_2-CLA derivatives.

2.5. Analysis of NO_2-CLA and nitrogen oxide species

CLA-TAG + $NaNO_2$ reaction products in hexane (50 μL) were dried under a stream of nitrogen gas, and resuspended in 1 mL phosphate buffer 50 mM, pH 7.4 with 100 μM DTPA and 20 μM 2,3-diaminonaphthalene (DAN) in presence or absence of 0.8 mg/mL porcine pancreatic lipase. Then, samples were incubated at 37 °C under continuous magnetic agitation and aliquots were taken at 15, 30, 60, 120, 240 min. For the analysis of NO_2-CLA and 2,3-naphtotriazole (NAT), 20 μL aliquots were resuspended in 200 μL acetonitrile with 4 pmol NO_2-SA internal standard, and analyzed by HPLC-MS/MS.

For the analysis of NO_2^- and NO_3^-, 100 μL aliquots at each time point were mixed with 100 μL chloroform/methanol (1/1, v/v) vortexed at 15000 g for 5 min at 4 °C, and the supernatant was injected into an Eicom NOx analyzer ENO-30 (Amuza Inc, San Diego, CA, USA). This system used a post-column diazo coupling reaction (Greiss reaction) combined with HPLC using a NO-PAK separation column. NO_2^- was derivatized with Griess reagent generating a red diazo compound, and absorbance was quantitatively measured by spectrophotometric detection at 540 nm. NO_3^- was reduced to NO_2^- on a cadmium reduction column and derivatized with the same diazo coupling reaction. NO_2^- and NO_3^- concentration were determined using calibration curves generated with sodium nitrite and sodium nitrate standards.

For the analysis of $^{\bullet}NO$, 20–30 μL of CLA-TAG or CLA+ $NaNO_2$ reaction products in hexane were directly injected into a Model 280 Nitric Oxide Analyzer (NOA, Sievers Instruments, Boulder, CO, USA) with a purge vessel containing bubbling phosphate buffer 25 mM (pH 7.4). The system measured $^{\bullet}NO$ based on a gas-phase chemiluminescent reaction between $^{\bullet}NO$ and ozone (O_3). Calibration curves were performed by injection of rapid release $^{\bullet}NO$ donors.

2.6. HPLC-UV-Vis analysis

Gastric CLA-TAG and CLA derivatives were both analyzed by HPLC-UV-Vis using an Agilent 1200 Series HPLC system with an analytical C18 Luna column (2 × 100 mm, 5 μm, Phenomenex) maintained at 40 °C and a diode array detector (DAD). The CLA-TAG products were chromatographically resolved using a solvent system of acetonitrile/water 50/50 (v/v) containing 0.1% formic acid (solvent A) and isopropanol/acetonitrile 70/30 (v/v) containing 0.1% formic acid (solvent B), at 0.7 mL/min flow rate with the following gradient program: 70–100% solvent B (0–3 min); 100% solvent B (3–6 min) followed by 3 min re-equilibration at initial conditions. Instead, the CLA products were eluted with a 0.65 mL/min flow rate and a solvent system consisting of water containing 0.1% acetic acid (solvent A) and acetonitrile containing 0.1% acetic acid (solvent B), with the following gradient program: 35–100% solvent B (0–8 min); 100% solvent B (8–10 min) followed by 2 min re-equilibration at initial conditions.

2.7. HPLC-MS/MS analysis

To further characterize gastric products, selected UV–Vis fractions were collected and analyzed by HPLC-HR-MS/MS using a Vanquish UPLC system in tandem with a Q-Exactive hybrid quadrupole-Orbitrap mass spectrometer equipped with a HESI II electrospray source (Thermo Scientific). CLA-TAG derivatives were chromatographically resolved with a C18 Luna column (2 x 150 mm, 3 μm, Phenomenex) at a flow rate of 0.4 mL/min and with a post-column infusion of 50 μL/min of 10% ammonium acetate in acetonitrile (10 mM final). The mobile phases were 10% water in acetonitrile (solvent A) and ethyl acetate (solvent B), and the following gradient was used: 35–90% solvent B (0–10 min); 90% solvent B (10–13 min) to then reach the initial conditions in 0.5 min and re-equilibrate for an additional 1.5 min. Free CLA reaction products were evaluated using the column, solvents and gradient described above for the HPLC-UV-Vis analysis.

Electrospray ionization of gastric CLA-TAG derivatives was operated in positive mode, and the following parameters were used: auxiliary gas heater temperature 250 °C, capillary temperature 300 °C, sheath gas flow rate 20, auxiliary gas flow rate 20, sweep gas flow rate 0, spray voltage 4 kV, S-lens RF level 60 (%). Full mass scan analysis ranged from 300 to 1500 *m/z* at 17500 resolution. The main chromatographic peaks of CLA-TAG products as NH_4^+ adducts were selected and subjected to MS2 fragmentation (composition confirmed at the <2 ppm level). Instead, mass spectrometry analysis of gastric CLA products was operated in negative ion mode using the following parameters: auxiliary gas heater temperature 325 °C, capillary temperature 300 °C, sheath gas flow 45, auxiliary gas flow 15, sweep gas flow 2, spray voltage 4 kV, S-lens RF level 60 (%). Full mass scan analysis ranged from 150 to 600 *m/z* at 17500 resolution. Parallel Reaction Monitoring (PRM) of *m/z* 387.21 and *m/z* 324.21 were used for NO_2–ONO_2-CLA and NO_2-CLA identification and characterization, respectively. Manufacturer's recommended calibration solutions were used to calibrate the instrument in positive and negative mode.

Plasma extracts were analyzed by HPLC-MS/MS using a C18 Luna column (2 x 100 mm, 5 μm, Phenomenex), with a 0.65 mL/min flow rate, and mobile phases of water 0.1% acetic acid (solvent A) and acetonitrile 0.1% acetic acid (solvent B). Extracts were injected at 35% solvent B, followed by a linear increase in the organic phase to 100% over 10 min with 2 min re-equilibration at initial conditions. A QTRAP 6500+ triple quadrupole mass spectrometer (Sciex, Framingham, MA) was used in negative ion mode with the following parameters: declustering potential (DP) - 60 V, collision energy (CE) - 42 eV, entrance potential (EP) and collision cell exit potential (CXP) - 5 V, and source temperature of 650 °C. Quantitation of plasma NO_2-CLA was performed by stable isotopic dilution analysis using calibration curves in the presence of the [^{15}N]O_2-CLA internal standard and following MRM transitions 324.2/46 and 325.2/47 respectively.

NAT and NO_2-CLA were resolved using a C18 Luna column (2 × 20 mm, 5 μm, Phenomenex) at a 0.75 mL/min flow rate, with a gradient solvent system consisting of water containing 0.1% acetic acid (solvent A) and acetonitrile containing 0.1% acetic acid (solvent B). Samples were injected at 10% solvent B followed by a linear increase to 100% over 3.3 min. The organic phase was kept at 100% for another minute and followed by 0.8 min at initial conditions. The analysis was performed with an API 5000 triple quadrupole mass spectrometer (Applied Biosystems, San Jose, CA), equipped with an electrospray ionization source (ESI). NAT was analyzed in positive mode for a duration of 2 min using the MRM transition 170.1/115.1 and the following parameters: DP 100 V, EP 3, CXP 10, CE 35, curtain gas 25, ionization spray voltage 5500, GS1 70, GS2 65, and a temperature of 650 °C. At 2 min the polarity was switched to negative mode and NO_2-CLA was analyzed using the MRM transition 324.2/46 and the following parameters: DP - 75 V, EP - 10 V, CXP - 8 V, and CE - 35 eV. Quantitation

of NAT and NO_2-CLA was performed with an external and internal calibration curve in the presence of the internal standard NO_2-SA (MRM 328.2/46), respectively.

2.8. Statistical analysis

Values are expressed as means ± standard deviation and unpaired t-test was used for statistical significance (*$p < 0.05$).

3. Results

3.1. Gastric generation of fatty acid nitrate esters

Oral supplementation of NO_2^- and CLA in rodents and humans increases plasma levels of NO_2-CLA and modulates hemodynamic responses [12,21,29]. Since dietary CLA is principally esterified in triacylglycerols (TAG), gastric NO_2-CLA formation was evaluated in rats gavaged with sodium nitrite ($NaNO_2$) and a CLA-containing triglyceride (CLA-TAG) at a level relevant to human dietary consumption (Fig. 1A). Pentagastrin (*i.p.*) was first administered to stimulate acid secretion since the gastric pH of rats is more basic (~4.5) than humans (~1.5-2.5) during digestion [30]. The full MS chromatographic profile of gastric content lipid extracts in the positive ion mode (300–1500 *m/z* range) reveals principal peaks from 5 min to 8 min (Fig. 1B). Peak 1 corresponds to native CLA-TAG and peak 2 to NO_2-CLA-containing triglycerides (NO_2-CLA-TAG) (RT 6.14 min, *m/z* 893.7544). The more abundant peak 3 (RT 5.70 min) shows an *m/z* value of 956.7499 consistent with the ammonium adduct of a nitro-nitrate-containing CLA-TAG (NO_2–ONO_2-CLA-TAG, confirmed at the 1 ppm level). Structural information was obtained upon collision-induced dissociation (MS2) of this peak, with the formation of 7 major fragments, corresponding to two triglyceride and five diglyceride ions (Fig. 1C). The first odd mass triglyceride ion (*m/z* 829.7260) did not contain nitrogen atoms and corresponded to the neutral losses of nitrous acid, nitric acid, water, and ammonia $[M-(HNO_2)-(HNO_3)-(H_2O)-NH_3]^+$ with a further loss of water, generating *m/z* 811.7186. Fragmentation and acyl chain losses generated five diacylglyceride ions. The key structural ion (*m/z* 683.4829, $[M-(16:0)-NH_3]^+$) contains both –NO_2 and –ONO_2 groups and results from the initial loss of palmitate and ammonia. Further neutral losses of HNO_3 (*m/z* 620.4880) and HNO_2 (*m/z* 573.4864) from this diacylglyceride establish the presence of –ONO_2 and –NO_2 groups on the conjugated acyl chain. This is further confirmed by the presence of *m/z* 551.5023, corresponding to $[M-(NO_2\text{-}ONO_2\text{-CLA})-NH_3]^+$ that is generated by neutral losses of nitro-nitrate-CLA (NO_2–ONO_2-CLA) and ammonia.

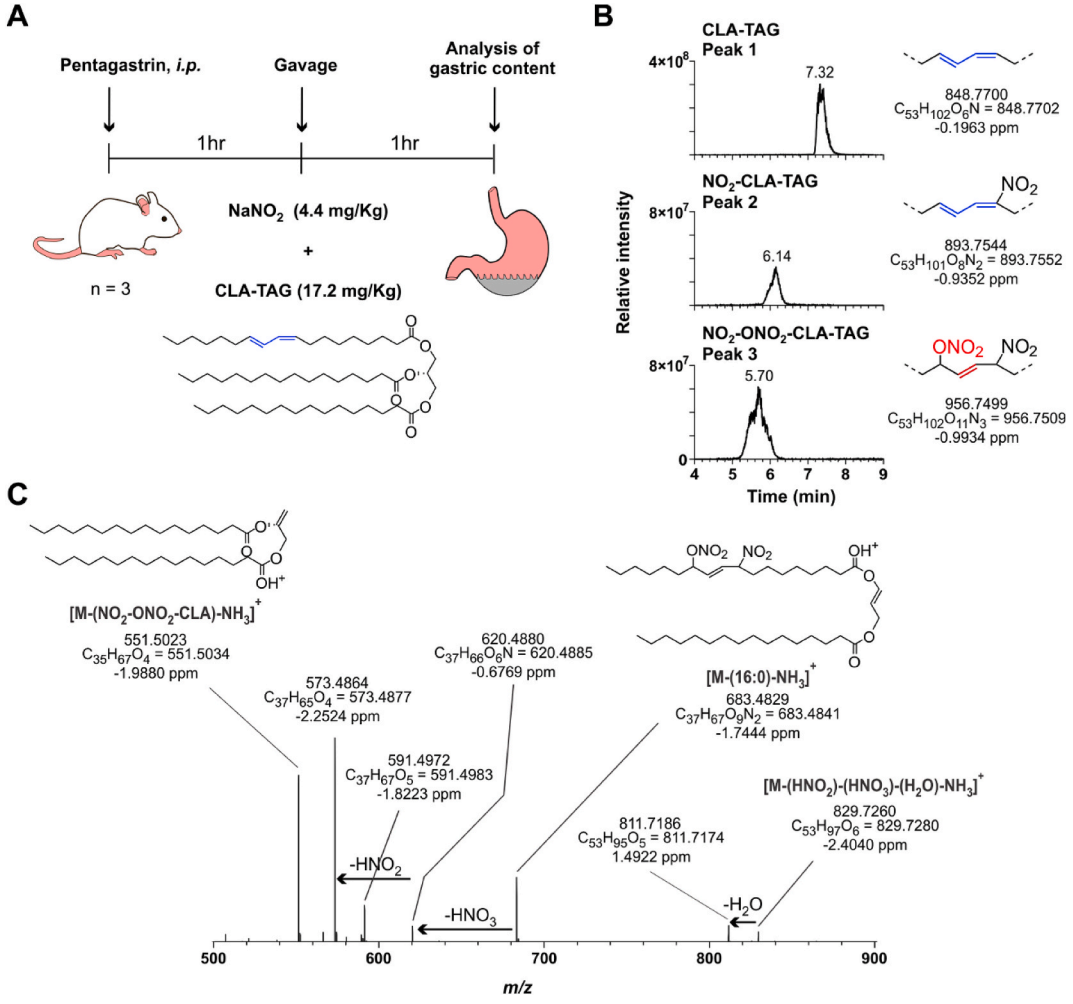

Fig. 1. Fatty acid nitro-nitrate esters are formed in the gastric compartment. (**A**) Schematic representation of treatment, supplementation, and recovery of gastric content in rats. (**B**) Mass chromatograms of gastric CLA-TAG (*m/z* 848.7), NO_2-CLA-TAG (*m/z* 893.7), and NO_2–ONO_2-CLA-TAG (*m/z* 959.7) as ammonium adducts $[M+NH_4]^+$, with elemental composition, theoretical mass, and mass accuracy. (**C**) MS2 spectrum of NO_2–ONO_2-CLA-TAG. Representative chemical structures are shown for the 9-NO_2-12-ONO_2-CLA-TAG regioisomers and corresponding product ions. Data are representative results from a pharmacokinetics study (n = 3).

3.2. In vitro generation and decomposition of NO_2–ONO_2

To further characterize NO_2–ONO_2-CLA generation, CLA-TAG and free CLA were incubated with $NaNO_2$ in artificial gastric fluid under aerobic conditions. Reaction products were analyzed by HPLC coupled to both a UV–Vis detector and a high-resolution mass spectrometer (HR-MS). In room air-equilibrated conditions, CLA-TAG + $NaNO_2$ reaction products show a principal 210 nm peak at 4.34 min (Fig 2A red and Suppl. Fig. 2A), a minor peak at RT 4.15 min, and unreacted CLA-TAG at 4.96 min (in grey) that coelutes with a synthetic standard (Fig. 2A lower trace). The late broad-eluting peak (RT 5.59 min) that follows the elution of CLA-TAG likely corresponds to trace dimerization products. Of note, product spectra have no 250–400 nm absorbance, indicating the absence of isolated (λ_{max} 257 nm) or conjugated nitroalkene groups (λ_{max} 312 nm) [25] (Suppl. Fig. 2C). HPLC-HR-MS analysis of the HPLC-UV fraction containing the main product peak (red) confirms the major formation of NO_2–ONO_2-CLA-TAG and only trace NO_2-CLA-TAG (Fig. 2B lower and upper panels in red). NO_2–ONO_2-CLA-TAG (*m/z* 956.7494) displays three chromatographic peaks at RT 5.91 min, 5.98 min, and 6.18 min, suggesting different regioisomers, while NO_2-CLA-TAG (*m/z* 893.7553) results in two peaks at RT 6.42 min and 6.5 min, corresponding to 12- and 9-NO_2-CLA-TAG, respectively [28]. In addition, minor dinitro-CLA-TAG, and oxidized-NO_2-CLA-TAG products were identified by atomic composition analysis with 2 ppm resolution (Suppl. Fig. 2E left panel).

The transit of gastric contents from the stomach to the duodenum occurs in concert with pH variations, increasing from acidic to neutral or slightly alkaline, and exposure to pancreatic secretions containing abundant lipase activities. To model this pH elevation, ammonium hydroxide was added to neutralize the reaction products formed by CLA-TAG or CLA and $NaNO_2$ in artificial gastric fluid (Fig. 2). UV chromatography profiling at 210 nm shows a main peak at 4.6 min that also strongly absorbs at 312 nm (Fig. 2A upper traces, blue and Suppl. Fig. 2B). The newly formed species both co-elutes and displays the same absorbance ratio 210nm/312nm = 1 (AUC_{210nm}/AUC_{312nm}) as a synthetic NO_2-CLA-TAG standard (Fig. 2A and Suppl. Fig. 1A). Mass analysis at the 2 ppm level confirms the atomic composition of NO_2-CLA-TAG (Fig. 2B upper panel in blue). Quantitation of the reaction products reveals that the primary species is NO_2–ONO_2-CLA-TAG (60 ± 13%) which, after addition of base, is stoichiometrically converted to NO_2-CLA-TAG (63 ± 11%), with 24 ± 11% corresponding to unreacted CLA-TAG (Fig. 2C). A set of minor products is also formed (RT 4.27 min), accounting for 7 ± 2% and consisting of oxidized-NO_2-CLA-TAG (Suppl. Fig. 2E central panel). Thus, *in vitro* nitration of free CLA under acidic gastric conditions confirms the formation of NO_2–ONO_2-CLA, that after neutralization with base, decays to NO_2-CLA (Suppl. Fig. 3). Quantitative analysis shows that NO_2–ONO_2-CLA accounts for 35 ± 11% of total products, with 5 ± 3% NO_2-CLA initially detected (Fig. 2D). The addition of base stoichiometrically converts NO_2–ONO_2-CLA to NO_2-CLA, representing 43 ± 23% of product. Additional structural insight comes

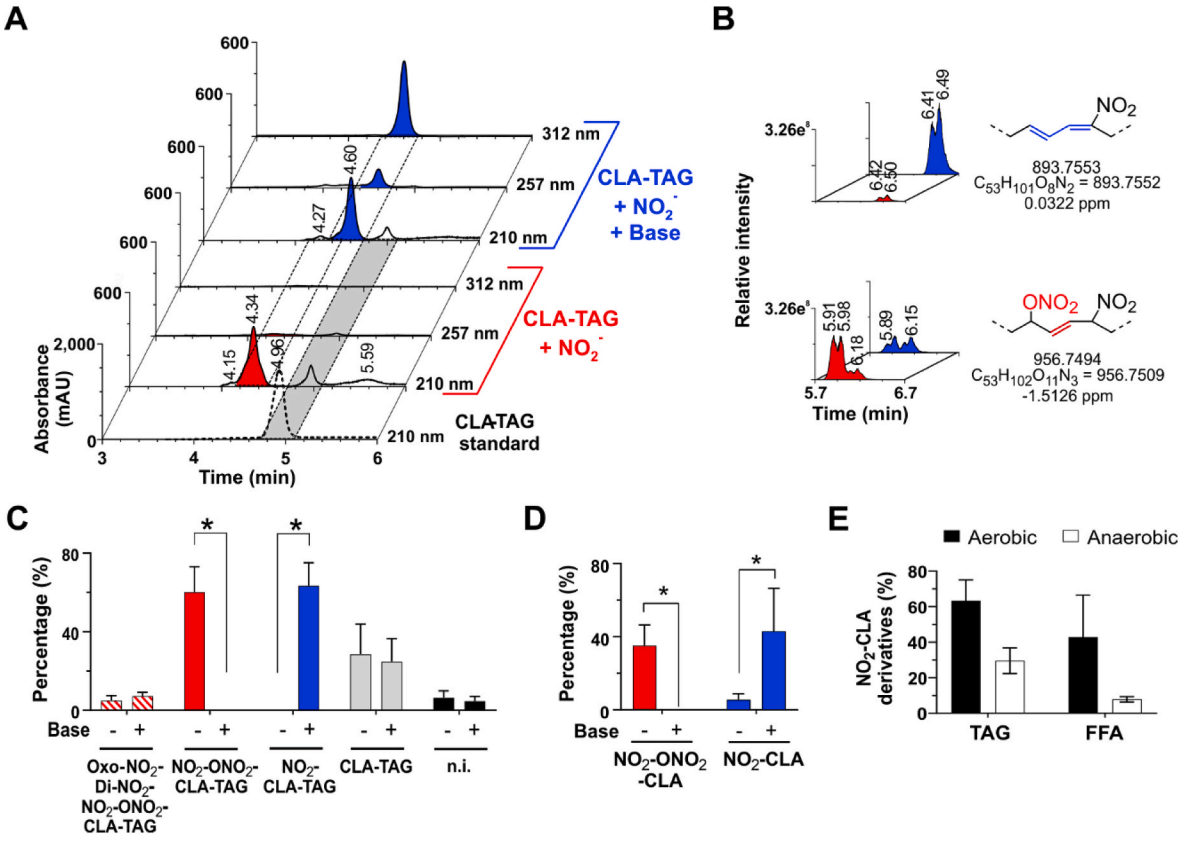

Fig. 2. Fatty acid nitration products formed by CLA-TAG and $NaNO_2$ in artificial gastric fluid - effect of pH and oxygen. (**A**) UV–Vis chromatograms of CLA-TAG and nitration products at 210 nm, 257 nm and 312 nm, before (in red) and after neutralization with base (blue). (**B**) HPLC-MS analysis of the UV–Vis fractionated peaks at 4.34 min (upper and lower panels in red) and 4.6 min (upper and lower panels in blue) before and after gastric fluid neutralization, respectively. The lower panel represents the mass chromatogram of NO_2–ONO_2-CLA-TAG (*m/z* 959.7) and the upper panel is NO_2-CLA-TAG (*m/z* 893.7), as ammonium adducts $[M+NH_4]^+$, with elemental composition, theoretical mass, and mass accuracy. Relative distribution of (**C**) CLA-TAG and (**D**) non-esterified CLA nitration products under aerobic conditions before and after addition of base. (**E**) Percentage of NO_2-CLA derivatives after base-catalyzed decay of esterified and free fatty acid (FFA) nitration products under aerobic and anaerobic conditions. Results were analyzed by an unpaired t-test (*$p < 0.05$). Data represents mean ± SD of 3 replicates from 3 independent experiments; n.i., non-identified. (For interpretation of the references to colour in this figure legend, the reader is referred to the Web version of this article.)

from infrared analysis of reaction products containing NO_2–ONO_2-CLA-TAG, that shows two characteristic peaks at 1633 cm^{-1} and 1555 cm^{-1} indicative of R–ONO_2 and R–NO_2 functional groups respectively [31] (Suppl. Fig. 4). After addition of base, the 1633 cm^{-1} peak is lost, and a new peak at 1515 cm^{-1} appears that corresponds to a vinyl-NO_2 group, reinforcing the formation of NO_2-CLA-TAG upon NO_2–ONO_2-CLA-TAG decay.

The stomach lumen is well oxygenated (~70 Torr, 7.6% O_2) compared with other compartments of the digestive tract [32]. The formation of products containing organic nitrates motivated evaluating the role of oxygen in the generation of NO_2–ONO_2-CLA species. Under anaerobic conditions, CLA-TAG + $NaNO_2$ products followed by HPLC-UV (λ_{210nm}) present a different profile than under aerobic conditions, yielding a peak at RT 4.24 min with a shoulder at RT 4.36 min, a main peak accounting for unreacted CLA-TAG and a minor peak at RT 5.37 min, that was not further characterized (Suppl. Fig. 5 A and C). MS analysis of the peak 1 fraction shows equal amounts of dinitro-CLA-TAG, oxidized-NO_2-CLA-TAG, and NO_2–ONO_2-CLA-TAG (Suppl. Fig. 5E). After base addition, the latter decomposed, generating NO_2-CLA-TAG at 4.61 min and a minor set of unidentified peaks (Suppl. Fig. 5B, D, E). Anaerobic conditions decrease the yield of NO_2–ONO_2-CLA-TAG (Suppl. Fig. 6A), and base-induced NO_2-CLA-TAG formation was ~50% lower than under aerobic conditions (Fig. 2E). Finally, the acidic nitration of CLA by NO_2^- under anaerobic conditions gives a significantly lower yield of NO_2–ONO_2-CLA which, in combination with unidentified species, accounted for 14 ± 3% of the reaction products and minimal NO_2-CLA (1.3 ± 0.4%) (Suppl. Fig. 6B and 7A, C, E). Addition of base further evidenced the presence of unidentified species that showed an absorbance ratio 210nm/312nm > 1 (Suppl. Fig. 7B peak 3). Overall, NO_2-CLA accounted for 8 ± 1% of total products, showing an ~80% reduction of NO_2-CLA yield from CLA under anaerobic rather than aerobic conditions (Fig. 2E).

3.3. Base-catalyzed decay of NO_2–ONO_2-CLA

The alkaline-catalyzed decay of NO_2–ONO_2-CLA-TAG to NO_2-CLA-TAG and the mechanism of –ONO_2 elimination was characterized as a function of pH by following absorbance changes at 312 nm. Under acidic conditions, NO_2–ONO_2-CLA-TAG species were relatively stable with minimal absorbance changes at pH 5.8 (Fig. 3A). Increasing alkalinity increased rates of NO_2-CLA-TAG formation. Separately, the analysis of non-esterified NO_2–ONO_2-CLA reaction products revealed similar pH-dependent decomposition kinetics with the corresponding generation of NO_2-CLA. Under acid pH conditions (pH 5.8), NO_2–ONO_2-CLA was relatively stable, with increases in pH concomitantly increasing rates of NO_2-CLA formation (Fig. 3B). A scan of the absorption spectrum of NO_2–ONO_2-CLA from 250 nm to 400 nm confirmed an absence of nitroalkene absorbance at 312 nm (Fig. 3C red dotted line). Alkalization to pH 7.4 induced time-dependent formation of species absorbing at 312 nm (0–8 min) with a single isosbestic point at 375 nm. This confirms the generation of only NO_2-CLA during NO_2–ONO_2-CLA decay, without detection of any reaction intermediates.

The pKa for the formation of NO_2-CLA-TAG and NO_2-CLA is 6.9 and 7.3 respectively, calculated by plotting the initial rate of decay as % of maximum versus pH (Fig. 3 D and E). The base-catalyzed kinetics of NO_2–ONO_2-CLA-TAG decay in an aprotic solvent (acetonitrile) revealed a decrease of parent molecule (red) and a corresponding increase in the NO_2-CLA-TAG product (in blue) (Suppl. Fig. 8). This data supports that the decomposition of free and esterified NO_2–ONO_2-CLA species under alkaline conditions involves the deprotonation of the α-carbon (to the –NO_2 group) with consequent bond reorganization upon β- or δ-elimination of the –ONO_2 group depending on the two possible parent molecule regioisomers, yielding an electrophilic nitroalkene moiety (Fig. 3F).

3.4. NO_2–ONO_2-CLA-TAG decomposition yields reactive nitrogen oxides

Organic nitrates, such as NTG, activate soluble guanylate cyclase and induce vasodilation via the generation of an •NO precursor [33]. The release of nitrogen oxides (NOx) by NO_2–ONO_2-CLA-TAG in phosphate buffer pH 7.4, was evaluated in the presence or absence of pancreatic lipase. The temporal formation of NO_3^-, NO_2^-, NO_2-CLA and 2,3-naphtotriazole (NAT) was followed (Fig. 4), with NAT being the product of 2, 3-diaminonaphthalene (DAN) cyclization induced by nitrosating species (e.g., N_2O_3). Lipase activity accelerated the generation of NO_3^- during NO_2–ONO_2-CLA-TAG hydrolysis and decay in buffered aqueous solution (Fig. 4A), in contrast with similar decay rates in methanol (Fig. 3 A and B). At 240 min the decay reactions with and without lipase converged to a yield of ~0.75. The NO_2^- generation upon aqueous decay of NO_2–ONO_2-CLA-TAG gave ~10-fold lower yields than for NO_3^-, with

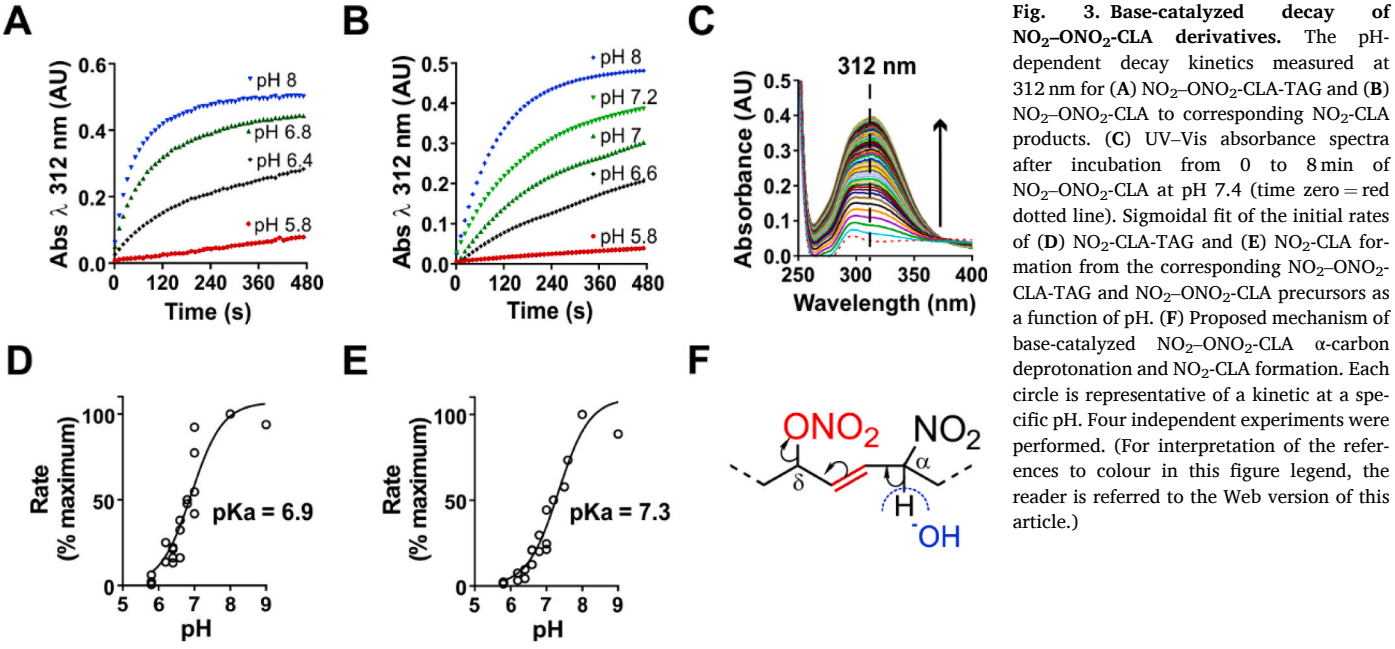

Fig. 3. Base-catalyzed decay of NO_2–ONO_2-CLA derivatives. The pH-dependent decay kinetics measured at 312 nm for (**A**) NO_2–ONO_2-CLA-TAG and (**B**) NO_2–ONO_2-CLA to corresponding NO_2-CLA products. (**C**) UV–Vis absorbance spectra after incubation from 0 to 8 min of NO_2–ONO_2-CLA at pH 7.4 (time zero = red dotted line). Sigmoidal fit of the initial rates of (**D**) NO_2-CLA-TAG and (**E**) NO_2-CLA formation from the corresponding NO_2–ONO_2-CLA-TAG and NO_2–ONO_2-CLA precursors as a function of pH. (**F**) Proposed mechanism of base-catalyzed NO_2–ONO_2-CLA α-carbon deprotonation and NO_2-CLA formation. Each circle is representative of a kinetic at a specific pH. Four independent experiments were performed. (For interpretation of the references to colour in this figure legend, the reader is referred to the Web version of this article.)

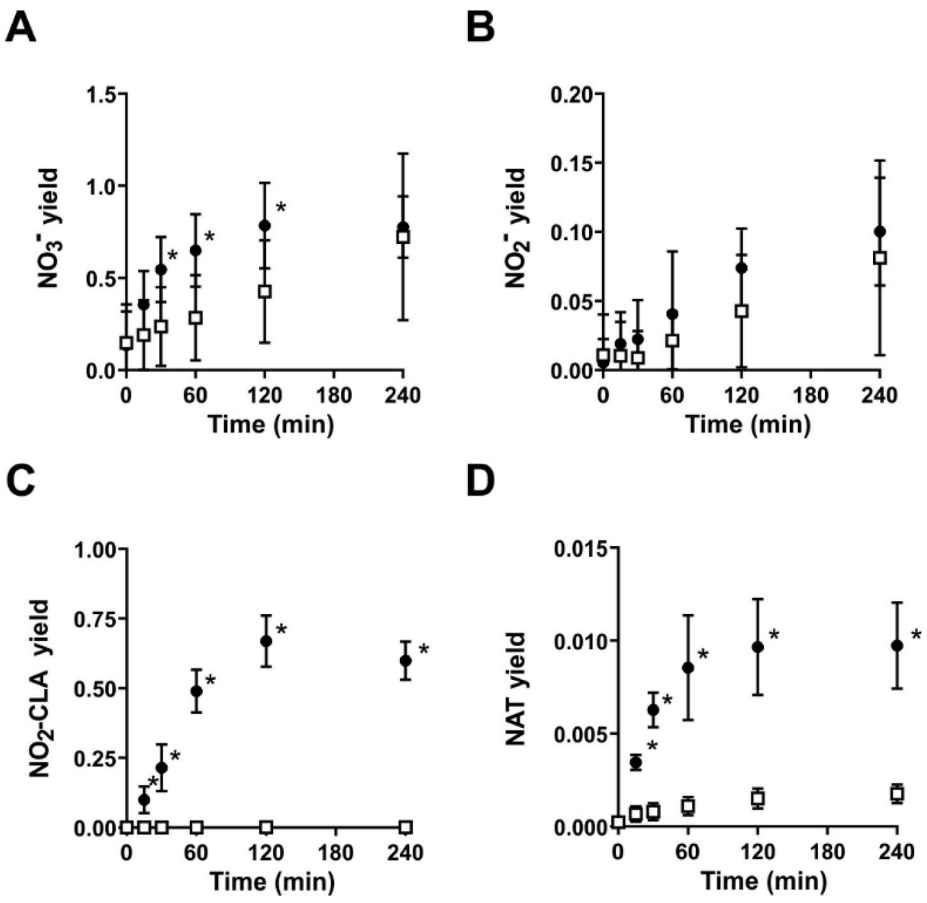

Fig. 4. Release of nitrogen oxides from NO_2–ONO_2-CLA-TAG decay. Time-dependent generation of (**A**) nitrate and (**B**) nitrite upon incubation of NO_2–ONO_2-CLA-TAG with porcine pancreatic lipase (black circles) or phosphate buffer (open squares). Decay of NO_2–ONO_2-CLA-TAG reaction products in presence of 20 μM 2,3-diaminonaphthalene (DAN) and porcine pancreatic lipase (black circles) or phosphate buffer (open squares) yields (**C**) NO_2-CLA and (**D**) nitrosative species detected as naphthalenetriazole (NAT) products. Yields are calculated as [product]/initial [NO_2–ONO_2-CLA-TAG]. Data represents mean ± SD of 3 replicates from 3 independent experiments with statistical significance (*$p < 0.05$) defined by two-way Anova and multiple comparison analysis.

no significant impact of lipase hydrolysis of TAG (Fig. 4B). Lipase hydrolysis of NO_2–ONO_2-CLA-TAG increased the rate of free NO_2-CLA yields with a similar kinetic profile and yield as for NO_3^- generation (Fig. 4C). In absence of lipase, no free NO_2-CLA is generated by the decay reactions of NO_2–ONO_2-CLA-TAG. Notably, lipase hydrolysis generated nitrosative species in yields greater than for the parent NO_2–ONO_2-CLA-TAG in neutral phosphate buffer and significantly lower than the other decay products (<1%) (Fig. 4D).

3.5. NO_2–ONO_2-CLA-TAG an in vivo precursor of NO_2-CLA

Having determined that gastric lipid nitration proceeds through unstable organic nitrate intermediates stabilized in triglycerides, we evaluated whether downstream NO_2–ONO_2-CLA products are stable in the alkaline intestinal environment and can be absorbed into the systemic circulation. Rats were treated with pentagastrin (*i.p.*) and gavaged with dietary levels of: 1) CLA-TAG + $NaNO_2$, 2) CLA-TAG, and 3) $NaNO_2$ (Fig. 5A). No NO_2–ONO_2-CLA-TAG species were detectable in plasma. Only plasma lipids from the group supplemented with CLA-TAG + $NaNO_2$ showed NO_2-CLA that was predominantly esterified (~13–18 to 1 ratio when compared to free acid) (Fig. 5B). At time zero, NO_2-CLA was undetectable and 1 hr after oral gavage of CLA-TAG + $NaNO_2$, free and esterified NO_2-CLA concentrations reached 2.44 ± 1.1 nM and 31.14 ± 15.05 nM, respectively. These plasma levels were maintained for 2 hr, followed by a 50% decrease at 4 hr.

4. Discussion

The stomach is a bioreactor that impacts both the reactions of NO_2^- and the spectrum of pleiotropic downstream systemic vasoregulatory and anti-inflammatory responses to this chemically-reactive species. These effects are predominantly acid-catalyzed, can be inhibited by proton pump inhibitors (e.g., esomeprazole) and mediated by secondary nitrogen oxides including $^{\bullet}NO$ and lipid electrophiles such as NO_2-FA [17,21,29,34]. Herein, we report that organic nitro-nitrate derivatives of unsaturated fatty acids are also generated in the acidic gastric compartment and characterize the physiological decomposition of NO_2–ONO_2-CLA derivatives into electrophilic NO_2-CLA and secondary nitrogen oxides.

Conjugated diene-containing triglycerides and NO_2^- (Fig. 1) are provided by a diet rich in dairy and plant oils, vegetables, and tubers. The latter two, rich sources of NO_3^-, provide mM levels of NO_2^- in the saliva upon NO_3^- reduction by oral bacterial nitrate reductases [4]. In the stomach's acidic pH (~1.2-2.5), NO_2^- is protonated to nitrous acid (HNO_2, pKa 3.4), a reaction that yields N_2O_3 and its products $^{\bullet}NO$ and $^{\bullet}NO_2$, proximal mediators of Cys nitrosation and unsaturated lipid nitration. In this regard, conjugated dienes of fatty acids, including CLA, are the preferential substrate for $^{\bullet}NO_2$-dependent nitration reactions, as opposed to bis-allylic moiety of fatty acids and protein tyrosine and tryptophan residues [12,35]. Finally, physiological gastric oxygen tensions (~70 Torr) [32] favor the formation of NO_2–ONO_2-CLA derivatives, in agreement with their greater *in vitro* yields under aerobic than anaerobic conditions (Fig. 2C and Suppl. Fig. 6A). These findings also underscore the possibility that NO_2–ONO_2-containing lipids can be generated in other acidic compartments, such as phagolysosomes, endosomes, and the intermembrane space of mitochondria.

When defining the potential ability for NO_2–ONO_2-CLA to gain systemic access upon transiting from the acidic gastric site of generation to the more alkaline intestine (pH ~6–8), it was discovered that at neutral to alkaline pH, both free and esterified NO_2–ONO_2-CLA were metastable non-electrophilic precursors of electrophilic NO_2-FA (Figs. 2 and 3). NO_2–ONO_2-CLA species are not electrophilic, lack the characteristic

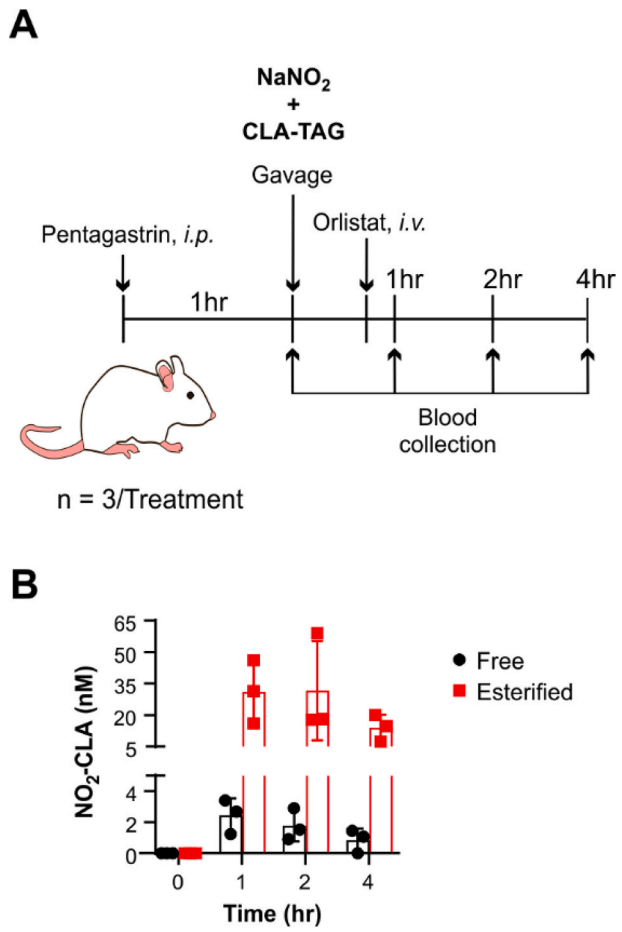

Fig. 5. Gastric NO_2–ONO_2-CLA-TAG derivatives are precursors of NO_2-CLA detected in systemic circulation. (**A**) Schematic representation of treatment protocol. (**B**) Free and esterified concentrations of NO_2-CLA in plasma of CLA-TAG + $NaNO_2$ gavaged rats.

nitroalkene absorbance peaks at ~260 nm, and are not a substrate for prostaglandin reductase 1 (PtGR-1), the enzyme that inactivates NO_2-FA signaling (Figs. 2A and 3F) [36]. Base-catalyzed NO_2–ONO_2-CLA decomposition and NO_2-CLA formation increased the absorbance at 312 nm, consistent with the electron delocalization present in the conjugated nitrodiene. It is anticipated that the activation of NO_2–ONO_2-CLA derivatives into electrophilic products could modulate characteristic signaling responses including inhibition of NF-kB-, toll--like receptor-4 (TLR4)- and protein stimulator of IFN genes (STING)--regulated pro-inflammatory cytokine and adhesion molecule expression, while activating adaptive HSF-1 and Nrf-2-regulated tissue-protective gene expression, thus impacting pathologic cell proliferation and tissue remodeling [5,37–39].

Organic nitrates induce soluble guanylate cyclase (sGc) activation, smooth muscle relaxation and vasodilation via mechanisms unrelated to direct $^{\bullet}NO$ release. For example, NTG undergoes diverse chemical reactions with heme proteins and oxidoreductases to yield NO_2^- and S-nitrosothiols [33,40]. NO_2–ONO_2-CLA derivatives have an acidic H (α to the electronegative –NO_2 group) with a pKa comparable to nitroalkanes in aqueous and methanol-water solutions [41,42] (Fig. 3). The alkaline-catalyzed α deprotonation induces a transient carbanion and subsequent electron migration, elimination of NO_3^- and formation of NO_2-CLA (Figs. 2-4). This mechanism is in agreement with the base-promoted loss of substituents on aliphatic compounds with α electron-withdrawing groups [43].

Nitrite generation may derive from decomposition mechanisms of NO_2–ONO_2-CLA derivatives via nucleophilic substitution of the –NO_2 group under neutral conditions [44] or alkaline deprotonation of the hydrogen α to the –ONO_2 group [45]. The detection of a nitro-keto-CLA-TAG product upon the base-catalyzed decay of NO_2–ONO_2-CLA-TAG in organic milieu supports this mechanism, that would yield a carbonyl product (Suppl. Fig. 2E). Nevertheless, the degradation of allyl-ONO_2 compounds or NO_2–ONO_2-containing lipids at different pH has not been characterized and we cannot exclude the possibility that both mechanisms may occur under neutral conditions. The lack of an effect of lipase on nitrite formation suggests that it is not primarily a result of hydrolysis of nitrosating species which might be responsible for DAN nitrosation (*e.g.*, N_2O_3, N_2O_4) (Fig. 4). Of note, sensitive ozone chemiluminescence analysis did not detect $^{\bullet}NO$ production by NO_2–ONO_2-CLA species in phosphate buffer at neutral and alkaline pH, arguing against $^{\bullet}NO$ autooxidation as a pathway for NO_2^- generation. This result also argues against the formation of gaseous nitrosative nitrogen oxides N_2O_3 or N_2O_4, since rapid stoichiometric homolysis upon volatilization [46] would produce detectable $^{\bullet}NO$. Further heavy isotope (^{15}N, ^{18}O)-based MS studies are required to unveil the mechanisms of formation and chemical nature of the nitrosative species detected upon lipase hydrolysis of NO_2–ONO_2-CLA-TAG (Fig. 4D).

To define potential *in vivo* NO_2–ONO_2-CLA-TAG signaling actions, we evaluated whether these gastric nitration products remain intact or are degraded into non-esterified NO_2-CLA by the combined effect of the more alkaline intestinal pH and pancreatic lipase hydrolysis. Fat absorption requires hydrolysis in the intestinal lumen followed by re-esterification into TAG and chylomicron transport and distribution to distal tissues [47]. Despite the use of the lipoprotein lipase inhibitor orlistat to increase chylomicron half-life, our attempts to detect circulating NO_2–ONO_2-CLA-TAG were unsuccessful [48]. The evaluation of NO_2–ONO_2-CLA-TAG in circulation is challenging because of an inherent instability in the strong conditions used for hydrolysis (Fig. 5). In addition, enterocyte re-esterification reactions result in scrambling of TAG fatty acids, further diluting NO_2–ONO_2-CLA in several different TAG species, precluding their detection *in vivo*.

Nitration of CLA occurs by the preferential addition of $^{\bullet}NO_2$ to the diene's external flanking carbons at positions 9 and 12 of the acyl chain, generating a nitrated allylic radical stabilized by electron resonance (Scheme 1). Under aerobic conditions, this intermediate can react with oxygen to generate a nitro-peroxyl radical, putatively reduced to a nitro-alkoxyl radical by oxidation of $^{\bullet}NO$ to $^{\bullet}NO_2$ [12]. Further reduction or oxidation of this nitro-alkoxyl radical can also form nitro-hydroxy-,

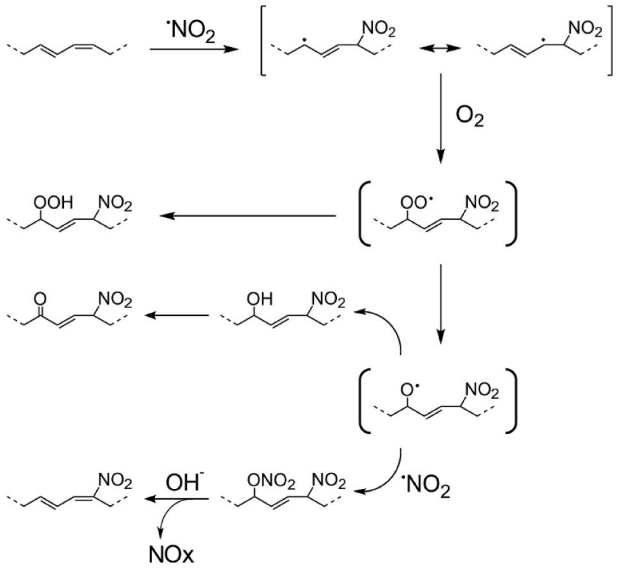

Scheme 1. Proposed mechanism for the reaction of $^{\bullet}NO_2$ with CLA moiety under aerobic conditions.

nitro-peroxy- or nitro-keto-CLA products. The present results reveal that NO_2–ONO_2-CLA derivatives are the principal gastric unsaturated fatty acid nitration products formed under aerobic conditions and suggest the reaction of $^{\bullet}NO_2$ with the nitro-alkoxyl radical in the generation of these species. On the contrary, in an oxygen-deficient environment, the initial reaction between the delocalized nitrated allylic radical and $^{\bullet}NO_2$ may generate a dinitro-CLA and an intermediate nitro-nitrito (NO_2–ONO) product [49]. The latter could release $^{\bullet}NO$ to form the central nitro-alkoxyl radical, which in turn could react with $^{\bullet}NO_2$ to yield lower levels of NO_2–ONO_2-CLA derivatives in comparison with aerobic conditions (Fig. 2E).

In conclusion, the reactions of dietary CLA and NO_2^- during digestion yield an endogenous nitrate ester, NO_2–ONO_2-CLA, that accounts for a new pathway leading to the endogenous generation of electrophilic NO_2-CLA. This intermediate can impact the plasma and tissue levels of NO_2-CLA because of increased stability of the nitro-nitrate ester in acidic gastric conditions and the suppression of a central route of nitro-fatty acid inactivation, the reduction of the nitroalkene by prostaglandin reductase-1. Further studies will reveal whether other acidic tissue compartments can generate NO_2–ONO_2-FA derivatives. Both endogenously-generated and exogenously administered NO_2–ONO_2-FA, having a functional group that is a key constituent of cardiovascular vasodilators, can potentially mediate $^{\bullet}NO$/cGMP-dependent signaling responses that may occur in the digestive tract or more remotely. It is shown herein that these signaling actions can occur in concert with the pleotropic cGMP-independent anti-inflammatory adaptive signaling actions that have been demonstrated for the fatty acid nitroalkene product formed by NO_2–ONO_2-CLA decay.

Author contributions

M.F. designed, performed and analyzed experiments, and wrote the manuscript. S.R.W. performed chemical synthesis of standards, NMR and IR analysis. P.R. performed *in vivo* experiments. K.R. and R.P. designed, performed and analyzed NO_2^-, NO_3^- and $^{\bullet}NO$ experiments. J.R. L. and D.A.V. designed experiments, contributed to data interpretation and provided critical insight into manuscript content. B.A.F. contributed to the overall concept, experimental design and manuscript preparation. F.J.S. designed experiments and contributed to data analysis and interpretation as well as manuscript writing.

Declaration of competing interest

F.J.S. and B.A.F. acknowledge an interest in Creegh Pharmaceuticals, Inc.

Acknowledgments

This work was financially supported by Ri.MED Foundation and NIH grants R21-NS112787 (MF), K01HL133331 (DAV), R01-HL058115, P30-DK072506, P01-HL103455 (BAF), R01-GM125944 and R01-DK112854 (FJS).

Appendix A. Supplementary data

Supplementary data to this article can be found online at https://doi.org/10.1016/j.redox.2021.101913.

References

[1] V.B. O'Donnell, et al., Nitration of unsaturated fatty acids by nitric oxide-derived reactive nitrogen species peroxynitrite, nitrous acid, nitrogen dioxide, and nitronium ion, Chem. Res. Toxicol. 12 (1999) 83–92.
[2] M. Delmastro-Greenwood, B.A. Freeman, S.G. Wendell, Redox-dependent anti-inflammatory signaling actions of unsaturated fatty acids, Annu. Rev. Physiol. 76 (2014) 79–105.
[3] J.O. Lundberg, E. Weitzberg, Biology of nitrogen oxides in the gastrointestinal tract, Gut 62 (2013) 616–629.
[4] J.O. Lundberg, E. Weitzberg, M.T. Gladwin, The nitrate-nitrite-nitric oxide pathway in physiology and therapeutics, Nat. Rev. Drug Discov. 7 (2008) 156–167.
[5] F.J. Schopfer, N.K.H. Khoo, Nitro-fatty acid logistics: formation, biodistribution, signaling, and pharmacology, Trends Endocrinol. Metabol. 30 (2019) 505–519.
[6] D.A. Vitturi, et al., Convergence of biological nitration and nitrosation via symmetrical nitrous anhydride, Nat. Chem. Biol. 11 (2015) 504–510.
[7] J.S. Beckman, T.W. Beckman, J. Chen, P.A. Marshall, B.A. Freeman, Apparent hydroxyl radical production by peroxynitrite: implications for endothelial injury from nitric oxide and superoxide, Proc. Natl. Acad. Sci. U. S. A 87 (1990) 1620–1624.
[8] S.V. Lymar, J.K. Hurst, Rapid reaction between peroxonitrite ion and carbon-dioxide - implications for biological-activity, J. Am. Chem. Soc. 117 (1995) 8867–8868.
[9] S. Goldstein, G. Czapski, Kinetics of nitric-oxide autoxidation in aqueous-solution in the absence and presence of various reductants - the nature of the oxidizing intermediates, J. Am. Chem. Soc. 117 (1995) 12078–12084.
[10] J.P. Eiserich, et al., Formation of nitric oxide-derived inflammatory oxidants by myeloperoxidase in neutrophils, Nature 391 (1998) 393–397.
[11] J.P. Eiserich, et al., Myeloperoxidase, a leukocyte-derived vascular NO oxidase, Science 296 (2002) 2391–2394.
[12] G. Bonacci, et al., Conjugated linoleic acid is a preferential substrate for fatty acid nitration, J. Biol. Chem. 287 (2012) 44071–44082.
[13] B.A. Freeman, V.B. O'Donnell, F.J. Schopfer, The discovery of nitro-fatty acids as products of metabolic and inflammatory reactions and mediators of adaptive cell signaling, Nitric Oxide : Biol. Chem. 77 (2018) 106–111.
[14] C. Mata-Perez, et al., Biological properties of nitro-fatty acids in plants, Nitric Oxide : Biol. Chem. 78 (2018) 176–179.
[15] M. Fazzari, et al., Olives and olive oil are sources of electrophilic fatty acid nitroalkenes, PloS One 9 (2014), e84884.
[16] C. Batthyany, et al., Reversible post-translational modification of proteins by nitrated fatty acids in vivo, J. Biol. Chem. 281 (2006) 20450–20463.
[17] L. Villacorta, et al., In situ generation, metabolism and immunomodulatory signaling actions of nitro-conjugated linoleic acid in a murine model of inflammation, Redox Biol. 15 (2018) 522–531.
[18] M.D. Resh, Covalent lipid modifications of proteins, Curr. Biol. 23 (2013) R431–R435.
[19] O. Rom, et al., Nitro-fatty acids protect against steatosis and fibrosis during development of nonalcoholic fatty liver disease in mice, EBioMedicine 41 (2019) 62–72.
[20] M. D'Ischia, Oxygen-dependent nitration of ethyl linoleate with nitric oxide, Tetrahedron Lett. 37 (1996) 5773–5774.
[21] M. Delmastro-Greenwood, et al., Nitrite and nitrate-dependent generation of anti-inflammatory fatty acid nitroalkenes, Free Radic. Biol. Med. 89 (2015) 333–341.
[22] A. Napolitano, E. Camera, M. Picardo, M. D'Ischia, Acid-promoted reactions of ethyl linoleate with nitrite ions: formation and structural characterization of isomeric nitroalkene, nitrohydroxy, and novel 3-nitro-1,5-hexadiene and 1,5-dinitro-1, 3-pentadiene products, J. Org. Chem. 65 (2000) 4853–4860.
[23] G.J. Buchan, G. Bonacci, M. Fazzari, S.R. Salvatore, S. Gelhaus Wendell, Nitro-fatty acid formation and metabolism, Nitric Oxide : Biol. Chem. 79 (2018) 38–44.
[24] F.J. Schopfer, C. Cipollina, B.A. Freeman, Formation and signaling actions of electrophilic lipids, Chem. Rev. 111 (2011) 5997–6021.
[25] S.R. Woodcock, S.R. Salvatore, G. Bonacci, F.J. Schopfer, B.A. Freeman, Biomimetic nitration of conjugated linoleic acid: formation and characterization of naturally occurring conjugated nitrodienes, J. Org. Chem. 79 (2014) 25–33.
[26] S.R. Woodcock, G. Bonacci, S.L. Gelhaus, F.J. Schopfer, Nitrated fatty acids: synthesis and measurement, Free Radic. Biol. Med. 59 (2013) 14–26.
[27] M. Fazzari, et al., Nitro-fatty acid pharmacokinetics in the adipose tissue compartment, J. Lipid Res. 58 (2017) 375–385.
[28] M. Fazzari, et al., Generation and esterification of electrophilic fatty acid nitroalkenes in triacylglycerides, Free Radic. Biol. Med. 87 (2015) 113–124.
[29] K.S. Hughan, et al., Conjugated linoleic acid modulates clinical responses to oral nitrite and nitrate, Hypertension 70 (2017) 634–644.
[30] E.L. McConnell, A.W. Basit, S. Murdan, Measurements of rat and mouse gastrointestinal pH, fluid and lymphoid tissue, and implications for in-vivo experiments, J. Pharm. Pharmacol. 60 (2008) 63–70.
[31] C.C. Lai, B.J. Finlayson-Pitts, Reactions of dinitrogen pentoxide and nitrogen dioxide with 1-palmitoyl-2-oleoyl-sn-glycero-3-phosphocholine, Lipids 26 (1991) 306–314.
[32] C.D. Koch, et al., Enterosalivary nitrate metabolism and the microbiome: intersection of microbial metabolism, nitric oxide and diet in cardiac and pulmonary vascular health, Free Radic. Biol. Med. 105 (2017) 48–67.
[33] L.J. Ignarro, et al., Mechanism of vascular smooth muscle relaxation by organic nitrates, nitrites, nitroprusside and nitric oxide: evidence for the involvement of S-nitrosothiols as active intermediates, J. Pharmacol. Exp. Therapeut. 218 (1981) 739–749.
[34] M.F. Montenegro, et al., Blood pressure-lowering effect of orally ingested nitrite is abolished by a proton pump inhibitor, Hypertension 69 (2017) 23–31.
[35] S.R. Salvatore, P. Rowart, F.J. Schopfer, Mass spectrometry-based study defines the human urine nitrolipidome, Free Radic. Biol. Med. (2020).
[36] D.A. Vitturi, et al., Modulation of nitro-fatty acid signaling: prostaglandin reductase-1 is a nitroalkene reductase, J. Biol. Chem. 288 (2013) 25626–25637.
[37] O. Rom, N.K.H. Khoo, Y.E. Chen, L. Villacorta, Inflammatory signaling and metabolic regulation by nitro-fatty acids, Nitric Oxide : Biol. Chem. 78 (2018) 140–145.

[38] A.J. Deen, et al., Regulation of stress signaling pathways by nitro-fatty acids, Nitric oxide Biol. Chem. 78 (2018) 170–175.
[39] A.L. Hansen, et al., Nitro-fatty acids are formed in response to virus infection and are potent inhibitors of STING palmitoylation and signaling, Proc. Natl. Acad. Sci. U. S. A 115 (2018) E7768–E7775.
[40] Z. Chen, J. Zhang, J.S. Stamler, Identification of the enzymatic mechanism of nitroglycerin bioactivation, Proc. Natl. Acad. Sci. U. S. A 99 (2002) 8306–8311.
[41] T. Matsui, L.G. Hepler, Acid ionizations of nitroalkanes in aqueous solution, Can. J. Chem. 51 (1973) 1941–1944.
[42] F.G. Bordwell, A.V. Satish, Is resonance important in determining the acidities of weak acids or the homolytic bond dissociation enthalpies (BDEs) of their acidic H-A bonds? J. Am. Chem. Soc. 116 (1994) 8885–8889.
[43] J.C. Fishbein, W.P. Jencks, Elimination reactions of beta-cyano thioethers: evidence for a carbanion intermediate and a change in rate-limiting step, J. Am. Chem. Soc. 110 (1988) 5075–5086.
[44] H. Chakrapani, M.J. Gorczynski, S.B. King, Allylic nitro compounds as nitrite donors, J. Am. Chem. Soc. 128 (2006) 16332–16337.
[45] C. Capellos, et al., Basic hydrolysis of glyceryl nitrate esters. I. 1-glyceryl and 2-glyceryl nitrate esters, Int. J. Chem. Kinet. 14 (1982) 903–917.
[46] B.C. Challis, S.A. Kyrtopoulos, Rapid formation of carcinogenic N-nitrosamines in aqueous alkaline solutions, Br. J. Canc. 35 (1977) 693–696.
[47] M. Fazzari, et al., Electrophilic fatty acid nitroalkenes are systemically transported and distributed upon esterification to complex lipids, J. Lipid Res. 60 (2019) 388–399.
[48] C.P. Pallasch, et al., Targeting lipid metabolism by the lipoprotein lipase inhibitor orlistat results in apoptosis of B-cell chronic lymphocytic leukemia cells, Leukemia 22 (2008) 585–592.
[49] W.A. Pryor, J.W. Lightsey, D.F. Church, Reaction of nitrogen dioxide with alkenes and polyunsaturated fatty acids: addition and hydrogen-abstraction mechanisms, J. Am. Chem. Soc. 104 (1982) 6685–6692.